Australian Government
Geoscience Australia

The Cooper Basin Region 3D Geological Map Version 1:

A search for hot buried granites

Tony Meixner and Fiona Holgate

Record
2009/15

GeoCat # 68823

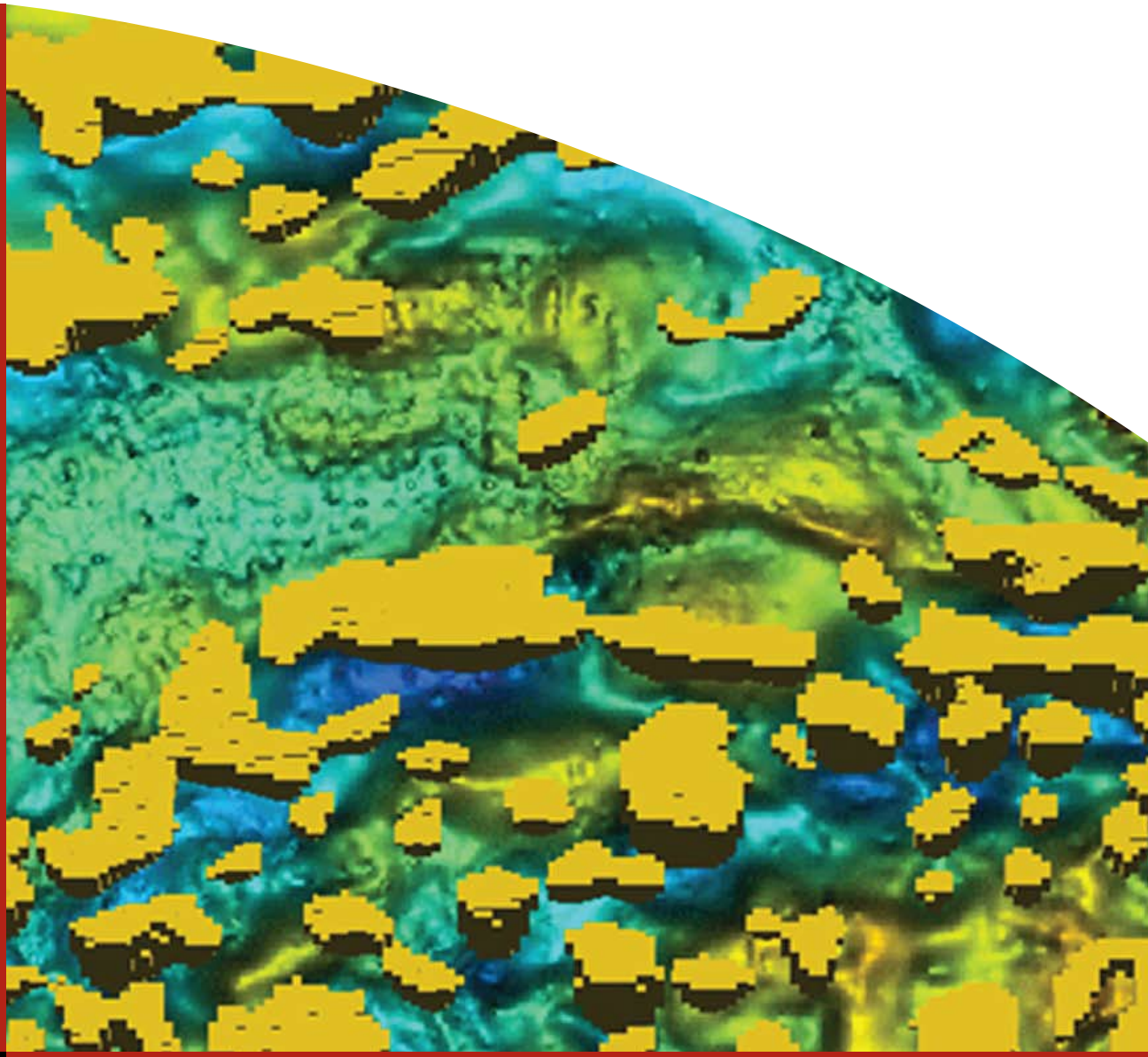

The Cooper Basin Region 3D Map Version 1: A Search for Hot Buried Granites

GEOSCIENCE AUSTRALIA
RECORD 2009/15

by

Tony Meixner[1] and Fiona Holgate[2]

Australian Government
Geoscience Australia

1. Geoscience Australia, GPO Box 378, Canberra ACT 2601
2. KUTh Energy Ltd., Level 57 MLC Centre, 19-29 Martin Place, Sydney NSW 2000

Department of Resources, Energy and Tourism
Minister for Resources and Energy: The Hon. Martin Ferguson, AM MP
Secretary: Mr John Pierce

Geoscience Australia
Chief Executive Officer: Dr Neil Williams PSM

ISSN 1448-2177
ISBN 978-1-921498-68-8 web
ISBN 978-1-921498-77-0 hardcopy

GeoCat # 68823

Bibliographic reference: Meixner, A. J. & Holgate, F., 2009. The Cooper Basin Region 3D Map Version 1: A Search for Hot Buried Granites. *Geoscience Australia, Record,* **2009/15**. 14p.

Contents

Executive Summary

A 3D map of the Cooper Basin region has been produced from 3D inversions of Bouguer gravity data using geological data to constrain the inversions. The 3D map delineates regions of low density within the basement of the Cooper/Eromanga Basins that are inferred to be granitic bodies. This 3D data release constitutes the first version 3D map of the Cooper Basin region. A future data release (version 2) will extend the area to the north and east to encompass the entire Queensland extension of the Cooper Basin and will incorporate more detailed 3D maps of the Cooper and Eromanga Basins. In addition, thermal properties will be incorporated into the 3D map to produce a 3D thermal model.

The Cooper Basin region is coincident with a prominent geothermal anomaly and forms part of a broad area of anomalously high heat flow. High-heat-producing granites, including granodiorite of the Big Lake Suite (BLS) at the base of the Cooper and Eromanga Basins sequences combined with thick Cooper/Eromanga sedimentary sequences that provide a thermal blanketing effect, results in temperatures as high as 270° C at depths <5 km. The location and characteristics of other granitic bodies are poorly understood and accurately identifying them is an important first step towards future geothermal exploration in this region.

3D Bouguer gravity field inversion modelling was carried out using the UBC inversion software. An initial gravity inversion was performed using seismic horizons to constrain the 3D distribution of the Cooper/Eromanga Basin sediments. Densities, derived from seismic velocities from a refraction seismic survey in the region, were assigned to the Cooper/Eromanga sediments in order to constrain their gravity contribution. A series of Iso-surfaces were generated, enclosing low density lobes within the basement of the initial sediment-constrained inversion model. Gravity 'worms' were used to pick the iso-surfaces that approximate the lateral sub-sediment extent of potential granites within the basement. A series of subsequent granite-constrained inversions were generated by assigning three different densities and maximum cut-off depths to the lobes. The inversion model that produced the most 'neutral' result had granite densities of 2.6 g cm^{-3} and a maximum cut-off depth of 12 km.

A smaller region was extracted from the Cooper Basin 3D map to be used as a test-bed for thermal modelling. Forward predictions of temperatures, vertical heat flow, vertical and total horizontal temperature gradient ware generated on a discretised model within GeoModeller. Inputs into the model consisted of mean annual surface temperature, basal heat flow, heat production and thermal conductivity for each lithology.

The 3D map shows a large volume of granitic material exists within the basement, a number of which correspond to high temperature anomalies in the predicted temperature at 5 km map, indicating that they have high-heat-producing compositions. The 3D map, which also defines the geometries of the Cooper and Eromanga Basins, therefore delineates both potential heat sources and thermally insulating cover and can be used as a predictive tool for delineating potential geothermal plays.

Introduction

A 3D Map of the Cooper Basin region has been produced over an area of 300 x 450 km to a depth of 20 km (Figure 1). The 3D map was constructed from 3D inversions of Bouguer gravity data, using geological data to constrain the inversions. The 3D map delineates regions of low density within the basement of the Cooper/Eromanga Basins that are inferred to be granitic bodies. This interpretation is supported by spatial correlations between the modelled bodies and known granite occurrences in the area. The 3D map, which also delineates the 3D geometries of the Cooper and Eromanga Basins, therefore incorporates both potential heat sources and thermally insulating cover: key elements in generating a geothermal play. This study was conducted as part of Geoscience Australia's Onshore Energy Security Program, Geothermal Energy Project.

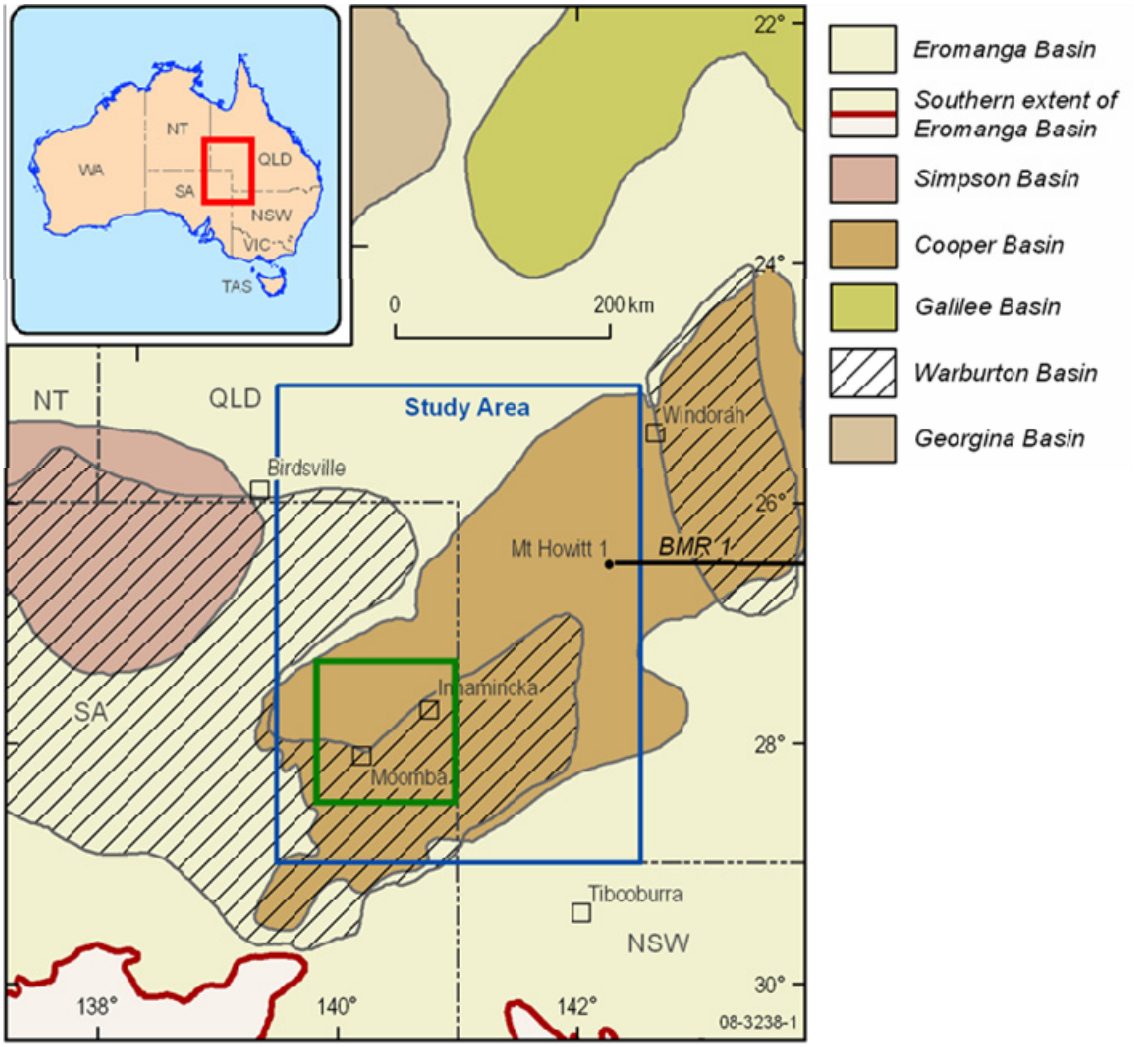

Figure 1: *Location of the Cooper Basin region, showing the spatial extents of the stacked Warburton, Cooper and Eromanga Basins. The outer blue outline indicates the extents of the Cooper Basin 3D model, the inner green outline indicates the extents of the thermal test model.*

The Cooper Basin region straddles the Queensland/South Australia (SA) border (Figure 1) and is coincident with a prominent geothermal anomaly (Cull & Denham, 1979; Cull & Conley, 1983; Somerville et al., 1994) (Figure 2). The region forms part of a broad area of anomalously high heat flow, which is attributed to Proterozoic basement enriched in radiogenic elements (Sass & Lachenbruch, 1979; McLaren et al., 2003). High-heat-producing granites, including granodiorite of the Big Lake Suite (BLS) at the base of the Cooper/Eromanga sequences, form a significant geothermal play that was targeted to be Australia's first Hot Rock development at Habanero (near Innamincka in SA). The relationship between high heat flow, high temperature gradient and anomalous heat production in the BLS is well established (Middleton, 1979; Gallagher, 1988; Beardsmore, 2004). The thick sedimentary sequences of the overlying Cooper/Eromanga Basins provide a thermal blanketing effect resulting in temperatures as high as 270° C at depths <5 km (Holgate, 2005). There is a good probability that analogous geothermal plays exist in association with other granitic bodies lying beneath the Cooper/Eromanga Basins. For the most part, the location and characteristics of these bodies are poorly understood and accurately identifying them is an important first step towards future geothermal exploration in this region.

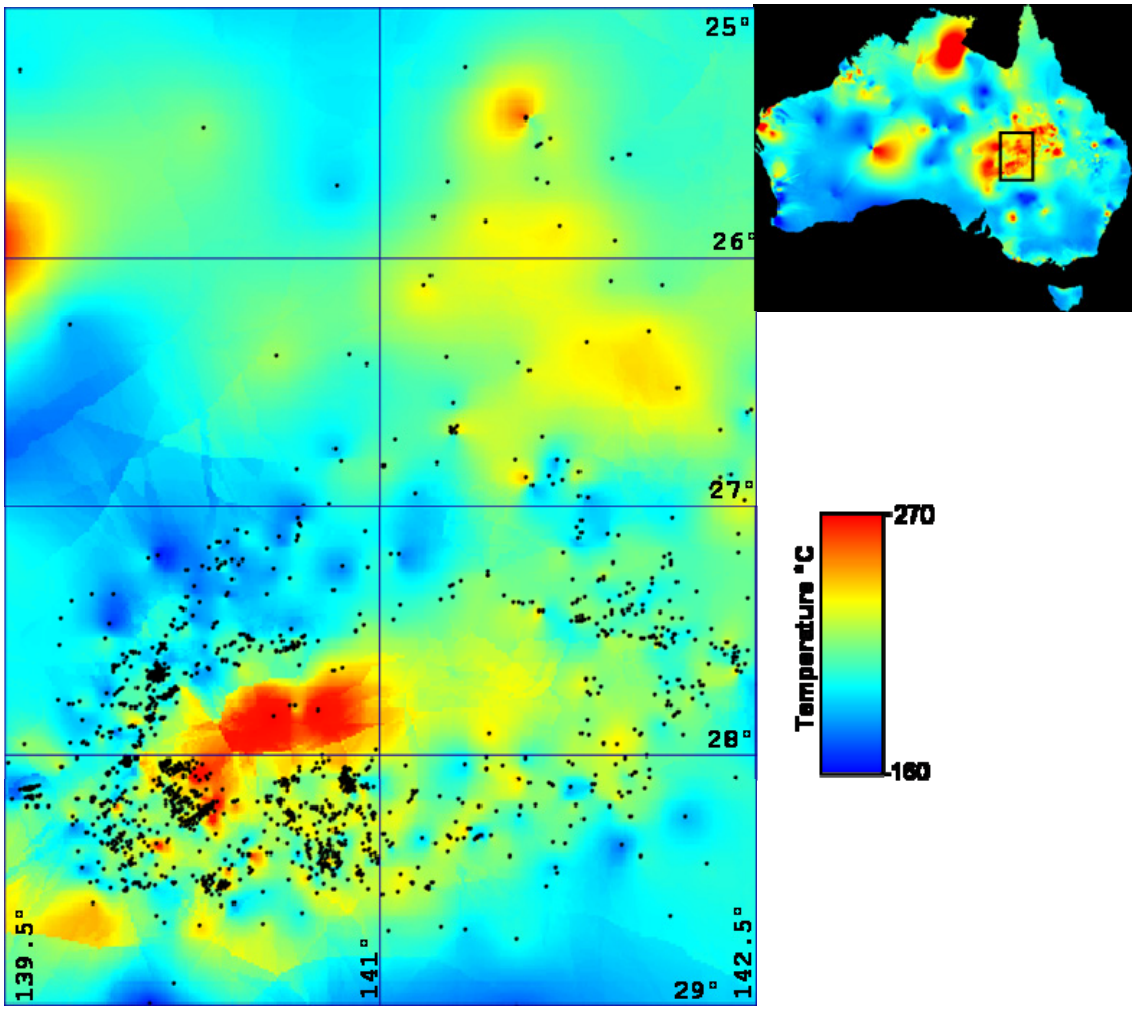

Figure 2: *Predicted temperature at 5 km map of Chopra & Holgate (2005), including the well locations.*

This 3D data release constitutes the first version 3D map of the Cooper Basin region. A future data release (version 2 of the 3D map) will extend the area to the north and east to encompass the entire Queensland extension of the Cooper Basin. On completion, the version 2 3D map will incorporate more detailed 3D maps of the Cooper and Eromanga Basins, by delineating the major internal sedimentary sequences within the basins. In addition, thermal properties will be incorporated into the 3D map to produce a 3D thermal model. The goal is to produce a 3D thermal model of the Cooper Basin region that not only matches existing temperature and heat flow data in the region, but also predicts regions of high heat flow and elevated temperatures in regions where no heat flow or temperature data exists.

An initial test-bed thermal model has been produced on a small portion of the Cooper Basin 3D map (Figure 1). The thermal modelling described herein is a work in progress and is being carried out to test the capability of the thermal modelling component of 3D GeoModeller, as well as our understanding of the thermal properties of the Cooper Basin region.

Geology of the Cooper Basin Region

The basement within the study area is completely obscured by successive sedimentary sequences of the Warburton, Cooper and Eromanga Basins. Basement drill intersections in the Cooper Region include Proterozoic gneisses to the north and south-east and Palaeozoic Tasmanides to the east (Gatehouse, 1986; Rankin & Gatehouse, 1990; Drexel et al., 1993).

The Cambro-Ordovician Warburton Basin formed as a result of marine incursion related to intra-continental rifting. The geology of the Warburton is summarised by Meixner et al. (1999) from studies including Gatehouse (1986), Gravestock and Gatehouse (1995), and Sun (1996; 1997; 1998). Basin sequences comprise volcanic and mixed sedimentary units overlain by carbonates, turbidites and a late red-bed unit. Sedimentation ceased in the late Ordovician and was followed by orogenesis during which burial depths are estimated to have reached 7-8 km (Sun, 1996, 1997; Boucher, 1994). In this study the Warburton Basin will be treated as basement due to its age, deformation history and depth of burial. This approach is supported by the absence of a gravity low associated with the Basin, suggesting that its density is comparable to that of underlying basement.

Granite intruded into Warburton sequences during orogenesis has been intersected in a number of wells (Figure 3). SHRIMP U-Pb zircon isotopic analyses from samples of BLS granodiorite indicate E. to Mid-Carboniferous crystallisation ages (Gatehouse et al., 1995). A density value of 2.6 g cm^{-3} was determined for the BLS by Boucher (1996). BLS drill intersections lie on a series of prominent circular gravity lows within a larger NE-trending low. A second (unnamed) granite of early Devonian age is recorded to the south of the BLS (Meixner et al., 1999). This intersection also coincides with a series of NNE-trending circular gravity lows.

The Warburton metasedimentary units and their intrusives are unconformably overlain by sequences of the L.-Carboniferous to Triassic Cooper Basin. Host to significant petroleum resources, the geology of the Cooper Basin is summarised in Meixner et al. (1999) from studies including Apak et al. (1997) and Kapel (1972). The south is dominated by NE trending structures including the Gidgealpa–Merrimelia–Innamincka (GMI) Ridge and the Nappacoongee–Murteree Ridge (NMR) which together separate the major depocentres of the

Patchawarra, Nappamerri and Tenappera Troughs (Figure 4). Vertical sediment thicknesses in the south are up to 2.5 km but decrease in the north. The unconformity at the base of the Cooper sequences is a prominent seismic marker mapped locally as the Z-horizon (Figure 4; PIRSA, 2008).

The Cooper Basin is unconformably overlain by sediments of the Jurassic to Cretaceous Eromanga Basin, with vertical thickness ranging from 1-3 km in the study area (Finlayson, 1988). The Cadna-owie Formation, a sandstone aquifer near the base of the Cretaceous, is a prominent feature mapped as the seismic C-horizon (PIRSA, 2008).

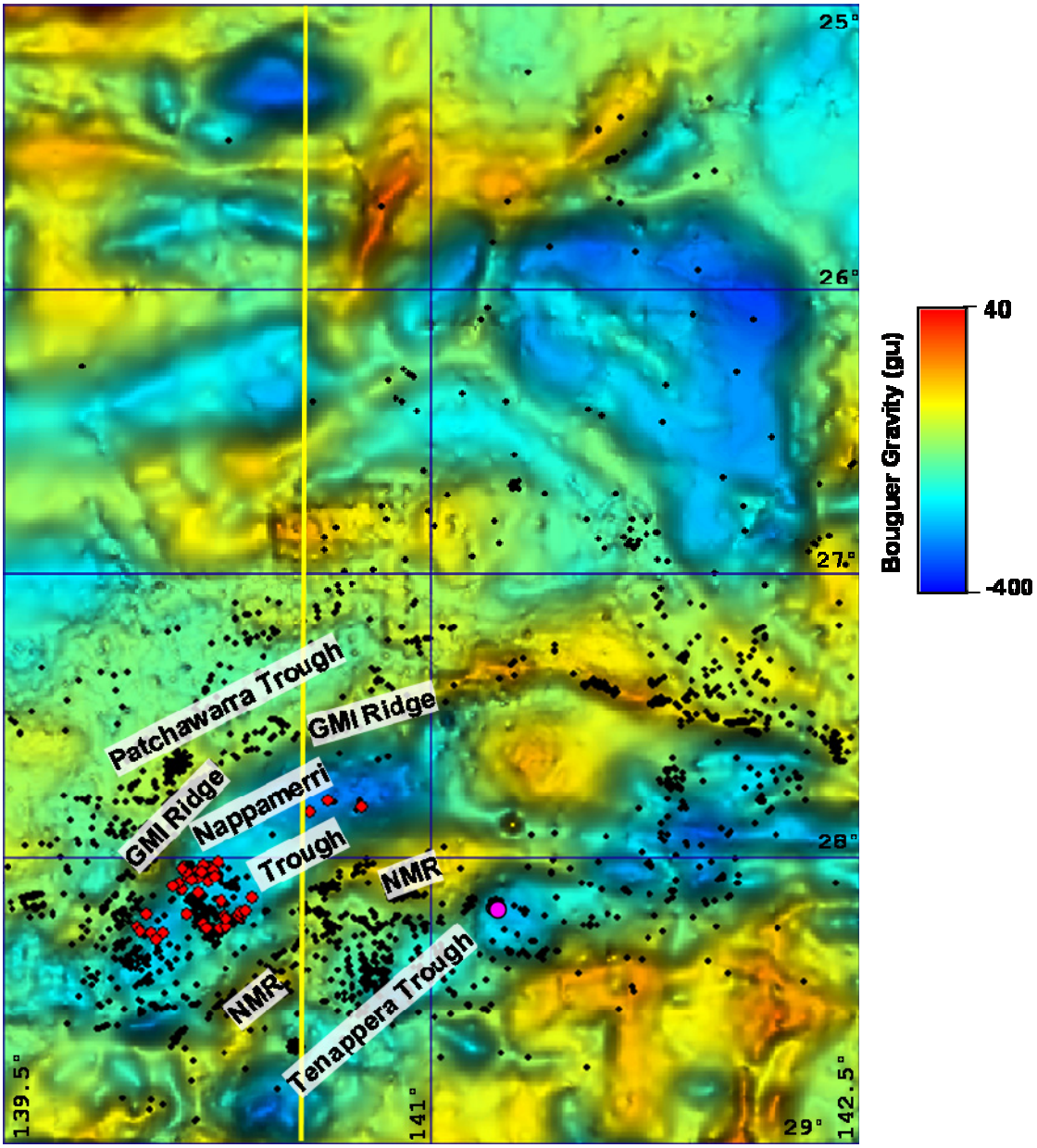

Figure 3: *Gravity image showing drill-hole locations (BLS intersections – red; early Devonian granite – pink). The major structural elements of the Cooper Basin and the location of the north-south section in Figure 5 (yellow) are also shown. GMI - Gidgealpa–Merrimelia–Innamincka; NMR - Nappacoongee–Murteree Ridge.*

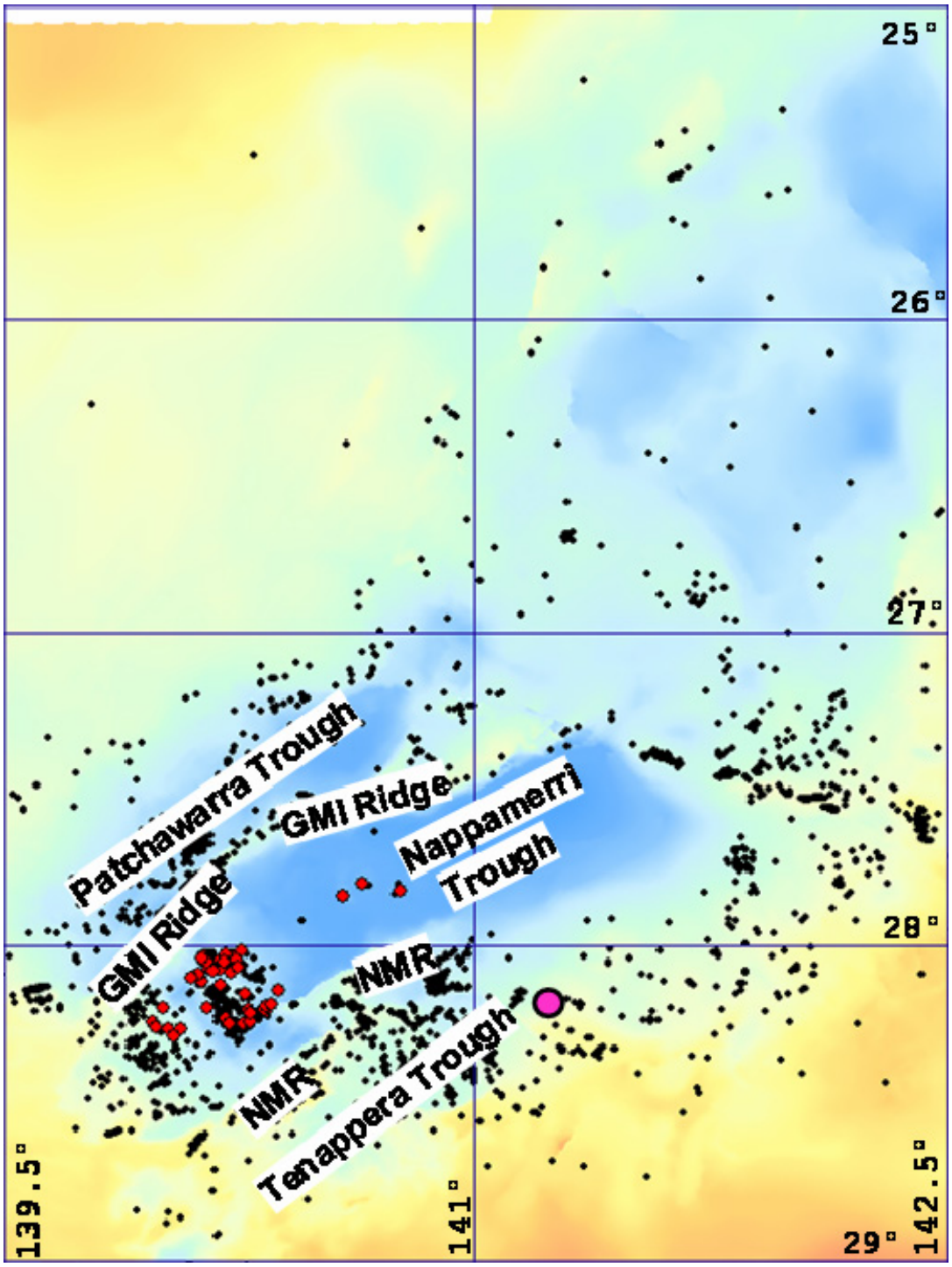

Figure 4: *Seismic Z-horizon image compiled from existing open file seismic sections, industry interpretations and 1300 well intersections (PIRSA, 2008). Within the extents of the Cooper Basin this surface represents the base of the Cooper sequences, outside this area it represents the base of the Eromanga sequence. The Z-horizon ranges from 815 m to 4496 m below the topography. Drill-hole locations (BLS intersections – red; early Devonian granite – pink) and major structural elements of the Cooper Basin are shown. GMI - Gidgealpa–Merrimelia–Innamincka; NMR - Nappacoongee–Murteree Ridge.*

Correlations of Gravity Data with Basin Structure

The Cooper region Bouguer gravity field is shown in Figure 3. Two NE to E-trending gravity lows broadly coincide with the Nappamerri and Tenappera troughs (Figure 4). These are bounded by NE to E-trending gravity highs which are similarly associated with the GMI Rise and NMR. In the NE of the study area, two prominent structural lows coincide with low gravity anomalies (Figures 3 and 4). There is thus a broad regional correlation between known basin structure and the gravity field, suggesting that the distribution of low-density basin-fill is of significance.

There is also evidence that density variations in the basement are contributing to the gravity field. Gravity lows that are coincident with the Nappamerri and Tenappera troughs extend beyond the trough boundaries (Figures 3 and 4). A number of intense, discrete gravity lows lie within the broader NE trends, in some cases coinciding with granite intersections in the Nappamerri and Tenappera Troughs. In the NW of the study area where the Eromanga Basin lies directly on basement, there are a number of prominent gravity lows that are not associated with any known basin structure. Finally, the gravity low coinciding with the Patchawarra Trough is of much lower amplitude than that of the Nappamerri Trough, even though the sediment thicknesses are similar. This suggests that the density composition of the basement beneath the troughs is different.

The gravity field is therefore influenced by both the thickness of basin sediment and by density variation in the basement. A goal of the gravity inversion is to constrain the influence of the basin sediments so that the density variation within the basement may be analysed.

3D Gravity Inversions

3D gravity field inversion modelling was carried out using programs developed by the University of British Columbia – Geophysical Inversion Facility (UBC-GIF) (Li and Oldenburg, 1998a). Iterative gravity inverse modelling is a process whereby adjustments are made to a density model, in the form of a mesh of rectangular prisms, until there is an acceptable fit between the predicted response of the model and the observed gravity data (Meixner & Lane, 2005). When geological and physical property observations are available, it is possible to make a reference model that will include geologically-sensible variations in the physical properties. The inversion can be forced to honour the supplied property values to within a specified upper and lower bound, at specific points within the model.

The inversion model consisted of a mesh with a cell size of 2 km lateral and 250 m vertical lengths. The resolution that can be achieved through inversion is ultimately dependent on the spacing and accuracy of the input gravity data. Given an average spacing between gravity observations of 4 to 7 km, it is unlikely that the use of cells smaller than 2 km would produce any additional information. The smaller vertical cell size used in this study was to accommodate the high resolution of the Z and C-seismic horizons that were used to constrain the model. The response of material beyond the limits of the inversion mesh was removed using the method described by Li and Oldenburg (1998b). The observed gravity data was then upward continued to 2 km: the same value as the horizontal length of the mesh cells.

CONSTRAINING THE BASIN SEDIMENTS

An initial gravity inversion was performed using the Z and C-seismic horizons to constrain the 3D distribution of the Cooper and Eromanga Basin sediments. These surfaces were incorporated into the mesh and a reference model was constructed. Density values were assigned to the individual cells of the reference model based on whether the centre of the cell falls below the Z-horizon (basement), between the Z and C-horizons (Z-C interval), and between the C-horizon and the topographic surface (C-topo interval).

The density values for the Z-C and C-topo intervals were generated from the results of a seismic refraction study along the BMR 1 traverse (Figure 1) in the central Eromanga Basin (Collins and Lock, 1990). P-wave refraction velocity data (V_p) was analysed for the shot point at Mount Howitt No. 1 well, which penetrated 1500 m of Eromanga and 900 m of Cooper Basin sediments. The V_p values for the intervals were averaged giving 3000 m s^{-1} for the C-topo and 43000 m s^{-1} for the Z-C intervals. The averaged V_p values were input into three functions that relates density to V_p. These functions consist of: (1) Gardners rule (Gardner et al., 1974); (2) the Nafe-Drake relationship generated by polynomial regression, as published in Brocher (2005) from a graphical relationship published in Ludwig et al., (1970) and; (3) Nafe-Drake relationship generated from polynomial regression, by Nick Direen (pers. comm.) from the graphical relationship published in Ludwig et al., (1970). The resulting densities matched to within 0.1 g cm^{-3} and were averaged to give a density of 2.3 g cm^{-3} for the C-topo interval and 2.5 g cm^{-3} for the Z-C interval.

The inversions were forced to honour the C-topo and Z-C densities to within ± 0.2 g cm^{-3} by specifying upper and lower bounds in the reference model. Although a density was assigned to the basement (2.67 g cm^{-3}), the corresponding upper and lower bounds (2.4 to 3.5 g cm^{-3}) were set such that they encompassed all likely rock densities (Emerson, 1990).

BUILDING THE 3D GRANITE-CONSTRAINED MAP

The inversion models of the basement have smooth variations in density. However, discrete boundaries can be constructed by producing 3D contour surfaces, termed iso-surfaces. A series of iso-surfaces were generated, based on a range of density values, enclosing successively larger regions of low density. The geometry of the regions are lobe-like with the maximum lateral extent at or near the top of the basement and gradually reducing in lateral extent at depth.

Gravity 'worms' were generated from the gravity data using the process described by Archibald et al. (1999). Gravity worms, or multi-scale edge mapping, is the process of mapping edges of source bodies in gravity data at a variety of scales. The worms are generated from the maxima in the horizontal gradient, and for the lower levels of upward continuation they approximate the position of the density contrast at the edge of a vertically dipping body. The lower level worms will, therefore, approximate the lateral sub-sediment extent of potential granites within the basement. Only those iso-surfaces with sub-sediment lateral extent that matched the lower levels of the worm data were selected.

A series of inversions were generated by assigning three different densities to the enclosed lobes in the reference model. The densities selected (2.55, 2.6 and 2.65 g cm^{-3}) cover a range of typical granite densities. The inversion was constrained by specifying ± 0.02 g cm^{-3} as upper and lower bounds in the reference model. A large portion of the low density lobes had total depths of less than 8 km. There were, however, a number of lobes coincident with the

more intense gravity anomalies with total depths considerably higher, up to 20 km. Granites with these larger depth extents were considered geologically unrealistic and were restricted by specifying a maximum cut-off depth for the low density lobes. Three additional reference models were generated for each of the above granite densities by assigning different levels of maximum cut-off depths of 8, 12, and 16 km.

Results of the nine inversions were analysed by inspecting the regions of the basement immediately below the base of the modelled granitic bodies. If the density of the granite in the reference model is too high and/or its depth extent is too low, then the inversion result will incorporate an anomalous region of low density in the basement directly beneath the modelled granite in order to satisfy the observed data. Conversely, if the density of the modelled granite in the reference model is too low and/or the depth extent too large, then an anomalous region of high density will be generated at the base of the granite. The inversion model that produced the most 'neutral' result had a density of 2.6 g cm^{-3} assigned to the modelled granites and a maximum cut-off of 12 km depth (Figure 5). The final 3D map of inferred sub-sediment granitic body distribution is shown in Figure 6.

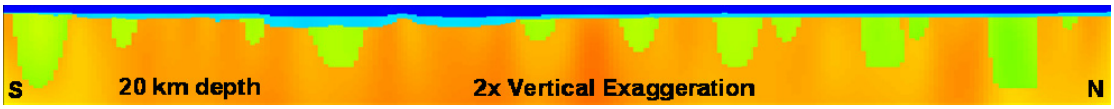

Figure 5: *North-south density section through the final gravity inversion model (see Figure 3 for location). The densities of the Eromanga Basin sediments (dark blue: 2.3 +/- 0.2 g cm-3), Cooper Basin sediments (light blue: 2.5 +/- 0.2 g cm-3) and the granitic bodies (green: 2.6 +/- 0.2 g cm-3) were constrained to a narrow density range, while the basement (yellow-red: 2.65-2.75 g cm-3) was left unconstrained.*

Thermal Modelling

A region 188 x 144 km by 16 km depth was extracted from the Cooper Basin 3D map to be used as a test region (Figure 1) for thermal modelling. Forward prediction of temperatures was generated on a discretised model within GeoModeller using the method described by Seikel et al. (2009). Temperatures were solved by explicit finite difference approximation using a Gauss-Seidel iterative scheme implemented until the sum of the residual errors fell below a specified threshold. Properties included in the output model consist of temperature (Figure 7), vertical heat flow, vertical temperature gradient and total horizontal temperature gradient.

To compute a thermal model the following inputs were required: mean annual surface temperature, basal heat flow, heat production of each lithology and thermal conductivity of each lithology. Initial values for these inputs were sourced from published literature (Beardsmore, 2004; Middleton, 1979) and assigned to the model. The results of the thermal modelling were compared to 21 bottom hole temperature (BHT) measurements (Chopra and Holgate, 2005), as well as 30 modelled 1D heat flow measurements (Beardsmore, 2004) from wells in the test area. A number of forward models were generated with varying inputs in order to minimise the temperature differences between the BHT and the modelled temperatures, as well as minimizing the difference between the measured and modelled heat flow measurements.

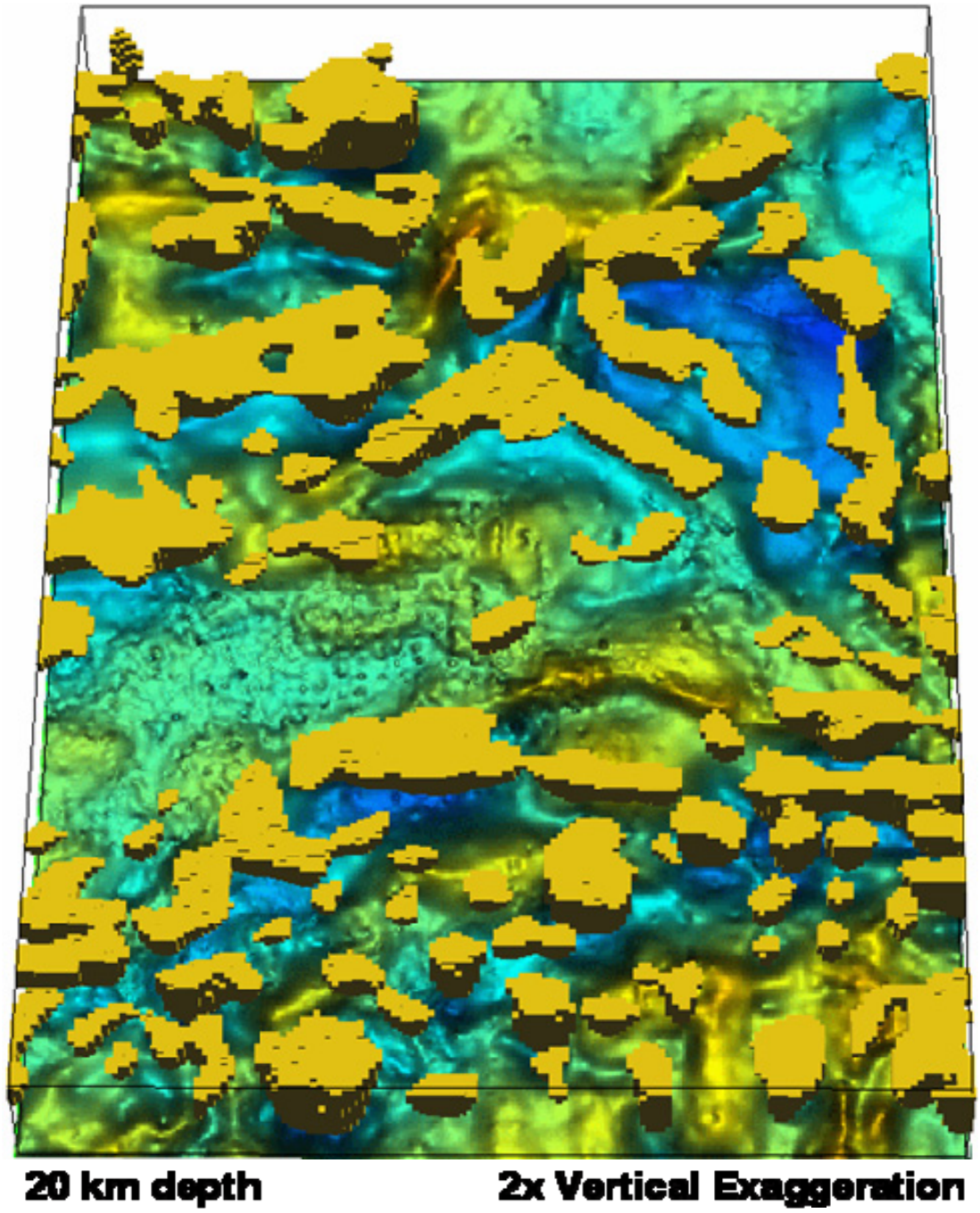

Figure 6: *3D model viewed obliquely from the south, of inferred sub-sediment granitic bodies, overlying an image of gravity data.*

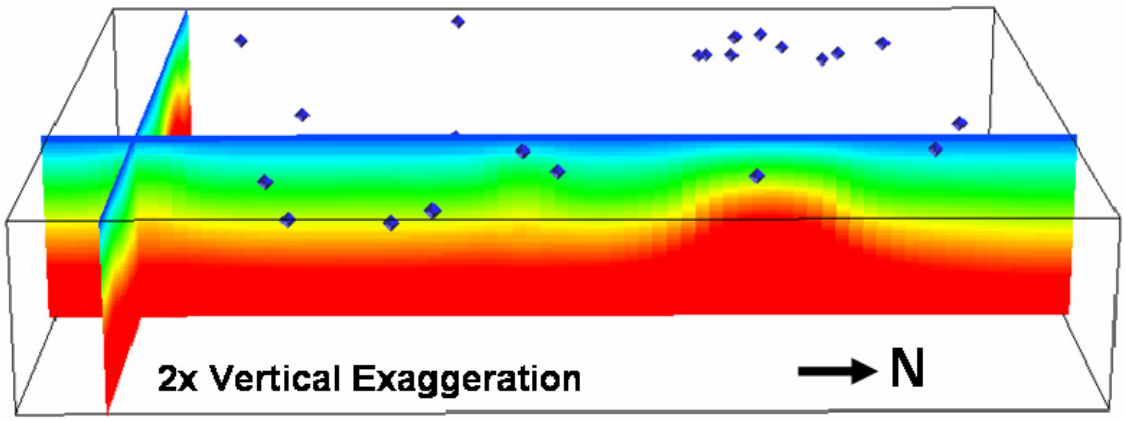

Figure 7: *Vertical sections through the test-bed temperature model showing the locations of the BHT well data. Temperatures range from 27° (blue) to 390° (red).*

Conclusion

The 3D map indicates that a large volume of granitic material exists within the basement. A number of these granite bodies, for instance the BLS granite (Figure 6), correspond to anomalies in the map of predicted temperature at 5 km, indicating that they likely have high-heat-producing compositions. A number of interpreted granite bodies do not correspond to temperature anomalies, indicating granite compositions which contain a range of radioelement concentrations.

The distribution of down-hole temperature measurements, from which the map of predicted temperature at 5 km is based, varies significantly in the study area (Figure 2) resulting in some temperature anomalies that are poorly constrained. The very high temperature anomaly coinciding with the intersected BLS, for example, is open to the east. The coincident mapped granite, however, defines an easterly limit for the BLS. The 3D map may also be used to predict potential thermal anomalies where no temperature measurements are available.

The 3D map, which also defines the geometries of the Cooper and Eromanga Basins, therefore delineates both potential heat sources and thermally insulating cover. In conjunction with the map of predicted temperature at 5 km depth, the 3D map can be used as a predictive tool for delineating potential geothermal plays.

Initial thermal modelling, although in its infancy, suggests that the 3D model can be assigned suitable estimates of thermal properties, to estimate the thermal composition of the Cooper Basin region, at least in the test area. It is expected that a more detailed 3D map of the Cooper and Eromanga sediments will produce a thermal model that will produce closer matches with the existing temperature and heat flow data.

REFERENCES

Apak, S. N., Stuart, W. J., Lemon N. M. and Wood, G., 1997. Structural evolution of the Permian-Triassic Cooper Basin, Australia; relation to hydrocarbon trap styles. *AAPG Bulletin,* **81(4)**. 533–555.

Archibald, N., Gow, P., and Boschetti, F., 1999. Multiscale edge analysis of potential field data. *Explor. Geophys.,* **30**. 38-44.

Beardsmore, G. R., 2004. Thermal modelling of the Hot Dry Rock geothermal resource beneath GEL99 in the Cooper Basin, South Australia. Sydney: 17th Aust. Soc. *Explor. Geophys. Conference*. Extended Abstracts.

Boucher, R. K., 1996. Big Lake Suite not Tirrawarra Sandstone in the Moomba Field, Cooper Basin, SA. *South Australia. Department of Mines and Energy. Report Book,* **96/31**. 1-5.

Brocher, T. M., 2005. Empirical relations between elastic wavespeeds and density in the Earth's crust. Bull. *Seismological Soc. America,* **95(6)**. 2081-2092.

Chopra, P. and Holgate, F. L., 2005. A GIS Analysis of Temperature in the Australian Crust. *Proceedings World Geothermal Congress 2005, Antalya, Turkey, 24-29 April 2005*.

Collins, C. D. N. and Lock, J., 1990. Velocity variations within the upper crustal basement of the central Eromanga Basin. *Bureau of Mineral Resources, Geology and Geophysics, Canberra. Bulletin*, **232**. 177-188.

Cull, J. P. and Denham, D., 1979. Regional variations in Australian heat flow. *Bureau of Mineral Resources, Journal of Australian Geology and Geophysics*, **4**. 1-13.

Cull, J. P. and Conley, D., 1983. Geothermal gradients and heat flow in Australian sedimentary basins. *Bureau of Mineral Resources, Journal of Australian Geology and Geophysics*, **8**. 329-337.

Drexel, J. F., Preiss, W. V. and Parker, A. J., 1993. The Geology of South Australia. Volume 1: The Precambrian. *South Australian Geological Survey Bulletin*, **54**.

Emerson, D. W., 1990. Notes on Mass Properties of Rocks – Density, Porosity, Permeability. *Explor. Geophys.*, **21**. 209-216.

Finlayson, D. M., Leven, J. H. and Etheridge, M. A, 1988. Structural styles and basin evolution in Eromanga region, eastern Australia. *AAPG Bulletin,* **72(1)**. 33-48.

Gallagher, K., 1988. The subsidence history and thermal state of the Eromanga and Cooper Basins. *PhD thesis, Australian National University*.

Gardner, G. H. F., Gardner, L. W. and Gregory, A. R., 1974. Formation velocity and density-the diagnostic basics for stratigraphic traps. *Geophysics*, **39**. 770-780.

Gatehouse, C. G., 1986. The geology of the Warburton Basin in South Australia: *Australian Journal of Earth Sciences*, **33(2)**. 161-180.

Gatehouse, C. G., Fanning C. M. and Flint, R. B., 1995. Geochronology of the Big Lake Suite, Warburton Basin, northeastern South Australia. *Quarterly Geological Notes – Geological Survey of South Australia,* **128**. 8-6.

Gravestock, D. I. and Gatehouse, C. G., 1995. Eastern Warburton Basin. In: J. F. Drexel and W. V. Preiss (Eds). Geology of South Australia, Volume 2, The Phanerozoic. *South Australia Geological Survey Bulletin*, **54**. 31-34.

Holgate, F., 2005. Exploration and Evaluation of the Australian Geothermal Resource. *PhD thesis, Australian National University*.

Kapel, A. J., 1972. The geology of the Patchawarra area, Cooper Basin. *APPEA Journa,*, **12(1)**. 53-57.

Li, Y., and Oldenburg, D. W., 1998a. 3-D inversion of gravity data. *Geophysics,* **63**. 109-119.

Li, Y., and Oldenburg, D. W., 1998b. Separation of regional and residual magnetic field data. *Geophysics,* **63**. 431-439.

Ludwig, W. J., Nafe, J. E. and Drake, C. L., 1970. Seismic refraction. In: A. E. Maxwell (Ed) The Sea, Vol 4, *Wiley-Interscience, New York*. 53-84.

McLaren, S., Sandiford, M., Hand, M., Neumann, N., Wyborn, L. and Bastrakova, I., 2003. The hot southern continent; heat flow and heat production in Australian Proterozoic terranes. In: R. R. Hills and D. R. Mueller (Eds) Evolution and dynamics of the Australian Plate. *Geol. Soc. of America Special Paper*, **372**. 157-167.

Meixner, A. J., Boucher, R. K., Yeates, A. N., Frears, R. A., Gunn, P. J. and Richardson, L. M., 1999. Interpretation of geophysical and geological data sets, Cooper Basin region, South Australia. *Australian Geological Survey Organisation, Record*, **1999/22**.

Meixner, A. J. and Lane, R., 2005. 3D Inversion of gravity data and magnetic data for the Tanami Region. Annual geoscience exploration seminar (AGES), 2005 – Record of abstracts. *Northern Territory Geological Survey, Record*, **2005-001**.

Middleton, M. F., 1979. Heat flow in the Moomba, Big Lake and Toolachee gas fields of the Cooper Basin and implications for hydrocarbon maturation. *Bulletin – Aust. Soc. of Exploration Geophysics,* **10(2)**. 149-155.

PIRSA, 2008. www.pir.sa.gov.au/petroleum/home/access_to_data/seismic_data/seismic_mapping/cooper_basin

Rankin, L. R. and Gatehouse, C. G, 1990. The northern margin of the Warburton Basin. Quarterly Geological Notes, *Geological Survey of South Australia*, **113**. 14-17.

Sass, J. H. and Lachenbruch, A. H., 1979. Thermal regime of the Australian Continental Crust. In: M. W. McElhinny (Ed) The Earth: its origin, structure and evolution. *Academic Press, London*, 301-351.

Seikel, R., Stüwe, K., Gibson, H., Bendall. B., McAllister, L., Reid, P., and Budd, A., 2009. Forward prediction of spatial temperature variation from 3D geology models. *Adelaide: 20th Aust. Soc. Explor. Geophys. Conference*. Extended Abstracts.

Somerville, M., Wyborn, D., Chopra, P., Rahman, S., Estrella, D. and Van der Meulen, T., 1994. Hot dry rock feasibility study. *Energy Research and Development Corporation, Report*, **94/243**. 133pp.

Sun, X., 1996. Sequence stratigraphy, Sedimentology, Biostratigraphy and palaeontology of the eastern Warburton Basin (Palaeozoic), South Australia. *National Centre for Petroloeum Geology and Geophysics, University of Adelaide*. PhD Thesis.

Sun, X., 1997. Structural style of the Warburton Basin and control in the Cooper and Eromanga basins, South Australia. *Explor. Geophys*., **28(3)**, 333-339.

Sun, X., 1998. Geochemistry and facies analysis of Cambrian volcanics in Warburton Basin and regional correlations, South Australia. Inaugural Sprigg symposium; the Ediacaran revolution; abstracts and programme. Sydney, N.S.W., Australia, *Geological Society of Australia*, **51**, 50.